# Pressure Dependence of the Crystal Structures and EPR Spectra of Potassium Hexaaquacopper(II) Sulfate and Deuterated Ammonium Hexaaquacopper(II) Sulfate

**Wolfgang Rauw,[†] Hans Ahsbahs,[‡] Michael A. Hitchman,*[,§] Sergei Lukin,*[,∥] Dirk Reinen,*[,†] Arthur J. Schultz,*[,⊥] Charles J. Simmons,*[,&] and Horst Stratemeier[§]**

Fachbereich Chemie und Zentrum für Materialforschung, Philipps Universität, Hans-Meerwein Strasse, D-35032 Marburg/Lahn, Germany, Fachbereich Geowissenschaft, Philipps Universität, Hans-Meerwein Strasse, D-35032 Marburg/Lahn, Germany, Chemistry Department, University of Tasmania, Box 252C, Hobart, Tasmania 7001, Australia, Donetsk Physicotechnical Institute of the National Academy of Sciences of the Ukrainian, Donetsk 340114, Ukraine, Intense Pulsed Neutron Source, Argonne National Laboratory, Argonne, Illinois 60439, and Mathematics and Science Division, Brigham Young University−Hawaii, Laie, Hawaii 96762

*Received July 7, 1995*[⊗]

The crystal structures of $(ND_4)_2[Cu(D_2O)_6](SO_4)_2$ at 295 K, determined by X-ray diffraction at pressures of 1 bar, ∼1.5 kbar and ∼3.0 kbar, are reported. Between 1 bar and 1.5 kbar, the crystal structure changes to one almost identical to that of the corresponding hydrogenous compound at 1 bar. The structural change involves a 90° switch in the direction of the long bonds of the $Cu(D_2O)_6^{2+}$ ion, accompanied by a change in the hydrogen-bonding interactions of the ammonium cations. Comparison of these two structures with those at ∼15 K shows that at room temperature, for both the high (**H**) and low (**L**) pressure phases, the Cu complexes are in thermal equilibrium with the other structural isomer. Though one of these is energetically preferred in the **H** and the other in the **L** phase, the variation of the powder EPR spectrum with pressure indicates a continuous transition between both within ∼1 kbar and suggests that at ∼0.5 kbar the two orientations of the copper complex are similar in energy. However, the underlying thermally induced equilibrium is little affected by pressure, and this is also the case for the $Cu(H_2O)_6^{2+}$ ion in $Cu^{2+}$-doped $K_2[Zn(H_2O)_6](SO_4)_2$. The crystal structure of $K_2[Cu(H_2O)_6](SO_4)_2$ at 15 K and 1.4 kbar, determined by time-of-flight neutron diffraction, is similar to that at 295 K and 1 bar, except for indications that here also a thermal population of the higher energy form in which the directions of the long and intermediate Cu−O bonds interchange occurs at 295 K. The powder EPR spectrum of the potassium salt at 295 K shows little change between 1 bar and 11 kbar.

## Introduction

The Jahn−Teller theorem provides the basic framework within which the stereochemistry and spectroscopic properties of $Cu^{2+}$ complexes are generally interpreted,[1] and interest in this area has recently increased with the suggestion that Jahn−Teller coupling may play a role in the mechanism underlying the behavior of high temperature superconductors involving this metal ion.[2] An unusual feature of copper(II) stereochemistry is the fact that the geometry and electronic structure of many complexes are temperature and/or pressure dependent.[3] Here, the geometric changes are normally observed by X-ray or neutron diffraction, while the electronic wave functions have been studied by **EPR** (electron paramagnetic resonance) spectroscopy.[4] A theoretical model was recently developed to interpret the properties of "fluxional" complexes of this kind. Initially, this was used to interpret the temperature dependent *g* values of 6-coordinate copper(II) complexes in terms of Jahn−Teller coupling and the influence of nonequivalent ligands,[5] though the model was subsequently extended to include the concomitant changes in the metal−ligand bond lengths.[6]

Particular interest has been shown in the copper(II) Tutton salts, of general formula $(cation)_2[Cu(H_2O)_6](SO_4)_2$. The fluxional behavior of the $Cu(H_2O)_6^{2+}$ group present when $Cu^{2+}$ is doped into the zinc(II) Tutton salts formed with a range of cations has been studied by EPR spectroscopy,[7,8,9] and similar dynamic behavior has been reported for undiluted $(NH_4)_2[Cu(H_2O)_6](SO_4)_2$.[10] The ammonium copper(II) Tutton salt is especially interesting because upon deuteration the long axis of the distorted $Cu(D_2O)_6^{2+}$ complex corresponds to a different pair of water molecules from that in the hydrogenous salt.[11] Also, when the pressure is raised from 1 bar to 1.5 kbar at 15 K, the structure of the deuterated compound alters to that of

[†] Fachbereich Chemie and Zentrum für Materialforschung, Philipps Universität.
[‡] Fachbereich Geowissenschaft, Philipps Universität.
[§] University of Tasmania.
[∥] Donetsk Physicotechnical Institute of the National Academy of Science of the Ukrainian.
[⊥] Argonne National Laboratory.
[&] Brigham Young University−Hawaii.
[⊗] Abstract published in *Advance ACS Abstracts,* March 1, 1996.

(1) Hathaway, B. J. *Struct. Bonding* **1984**, *57*, 55. Reinen, D.; Atanasov, M. *Magn. Reson. Rev.* **1991**, *15*, 167.
(2) Reinen, D.; Wegwerth, J. *J. Phys. C* **1991**, *183*, 261; Fil. D. V.; Tokar, O. I.; Shelankov, A. L.; Weber, W. *Phys. Rev. B* **1992**, *45*,5633 and references therein.
(3) Gazo, J.; Bersuker, I. B.; Garaj, J.; Kabesova, M.; Kohout, J.; Langfelderova, H.; Melnik, M.; Serator, M.; Valach, F. *Coord. Chem. Rev.* **1976**, *11*, 253.
(4) For a recent summary of work in these areas see: Hitchman, M. A. *Comments Inorg. Chem.* **1994**, *15*, 197.
(5) Riley, M.; Hitchman, M. A.; Reinen, D. *Chem. Phys.* **1986**, *102*, 11.
(6) Stratemeier, H.; Hitchman, M. A.; Bebendorf, J.; Reinen, D.; Gamp. E.; Bürgi, H. B. To be submitted for publication.
(7) Silver, B. L.; Getz, D. *J. Chem. Phys.* **1974**, *61*, 638.
(8) Petrashen, V. E.; Yablokov, Yu. V.; Davidovitch, R. L. *Phys. Status Solidi B* **1980**, *101*, 117.
(9) Riley, M. J.; Hitchman, M. A.; Wan Mohammed, A. *J. Chem. Phys.* **1987**, *87*, 3766.
(10) Alcock, N. W.; Duggan, M.; Murray, A.; Tyagi, S.; Hathaway, B. J.; Hewat, A. W. *J. Chem. Soc., Dalton Trans.* **1984**, 7.
(11) Hathaway, B. J.; Hewat, A. W. *J. Solid State Chem.* **1984**, *51*, 364.

0020-1669/96/1335-1902$12.00/0 

the hydrogenous compound,[12] the first known example of such a Jahn−Teller "switch".

At 1 bar, the distances observed for the two pairs of Cu−O bonds involved in this switch also change as a function of temperature,[11] implying that the two $Cu(D_2O)_6^{2+}$ polyhedron geometries are involved in a thermal equilibrium. This raises a number of questions as far as the pressure dependence of the structure is concerned. Assuming that a similar structural change to that observed when the temperature is lowered occurs, does this involve a gradual or sharp shift in the position of the equilibrium as a function of pressure? Does the structural change take place at the same pressure if this is approached from a high pressure or a low pressure, *i.e.* are any "hysteresis" effects apparent? To answer these questions we have measured the EPR spectrum of powdered $(ND_4)_2[Cu(D_2O)_6](SO_4)_2$ at ∼300 K over a range of pressures, and also performed crystal structure determinations at 295 K by X-ray diffraction at 1 bar, ∼1.5 kbar, and ∼3.0 kbar. The pressure dependence of the EPR spectrum of $Cu^{2+}$-doped $K_2[Zn(H_2O)_6](SO_4)_2$ has also been measured, to determine the effect of pressure on a complex which is known to exhibit a structural equilibrium as a function of temperature,[7,9] but where the lattice does not change significantly with pressure.

The compound $K_2[Cu(H_2O)_6](SO_4)_2$ has a similar structure to $(ND_4)_2[Cu(D_2O)_6](SO_4)_2$ at 1 bar.[13,14] To see whether the potassium salt undergoes a structural switch similar to that of $(ND_4)_2[Cu(D_2O)_6](SO_4)_2$ at high pressure, or a change in structure with temperature, the crystal structure was determined by time-of-flight neutron diffraction at 15 K and 1.4 kbar pressure and the EPR spectrum was measured between 1 atm and 11 kbar at 295 K. This paper presents the results of these studies.

## 1. Experimental Section

**1.1. Preparation of Compounds.** The procedure used to prepare crystals of $(cation)_2[Cu(H_2O)_6](SO_4)_2$, cation = K and $NH_4$, has been described previously,[15] as has the method of deuteration of the ammonium salt.[12]

**1.2. X-ray Structure Determinations at Different pressures.** For the single crystal measurements, a crystal of $(ND_4)_2[Cu(D_2O)_6](SO_4)_2$ was mounted in a high-pressure cell constructed by the method described by Merrill and Bassett,[16] as modified by Hazen and Finger.[17] This pressure cell limits the area over which data can be collected, leading to larger uncertainties of the structural data in the vertical direction. The crystal was therefore oriented in the cell in such a manner that the Cu−O7 and Cu−O8 bond lengths could be determined as precisely as possible, these lying approximately in the (001) plane of the unit cell. Deuterated isopropanol was used as the inert fluid to transmit the pressure. The increase in pressure was measured by monitoring the shift in wavelength of the $^2E \rightarrow {}^4A_2$ luminescence of a speck of ruby placed in the isopropanol, following the procedure of Barnett.[18] The line width limits the accuracy of the method to ∼0.5 kbar. The structure determination was carried out using a Stoe-AED-four-circle diffractometer with graphite monochromator and Mo Kα radiation. Experimental details are listed in Table 1. In addition to the standard corrections (absorption and Lorentz polarization corrections, peak profile analysis, averaging of symmetry equivalent reflexes and subtraction of background scattering) it was necessary to apply additional absorption corrections to compensate for the presence of the high pressure cell. The pathways of the X-rays in the diamond and beryllium parts of the pressure cell depend only on $|\omega|$ for the incoming and on $|2\theta - \omega|$ for the leaving beam, when working in the fixed $\phi$ mode.[17] The respective distances were estimated from a large-scale drawing of the cell, and the resulting correction factors applied to the measured intensities. Reflections with anomalous peak shapes due to diamond and ruby were omitted. Calculated and observed structure factors of the structures at 1 bar, ∼1.5 kbar, and ∼3.0 kbar are available as Supporting Table 1.

**Table 1.** Crystallographic Data for $(ND_4)_2Cu(SO_4)_2 \cdot 6D_2O$[a]

| | |
|---|---|
| Pressure = 1 atm | |
| $a = 9.296(1)$ Å | space group: monoclinic $P2_1/a$ (No. 14) |
| $b = 12.514(1)$ Å | $T = 295$ K |
| $c = 6.188(2)$ Å | $\lambda = 0.710\ 73$ Å |
| $\beta = 106.40(1)°$ | $V = 690.5(2)$ Å$^3$ |
| $Z = 2$ | |
| $R(F_o) = 18.9$ | $R_w(F_o) = 5.1$ |
| $R(F^2 > 3\sigma(F^2)) = 5.9$ | $R_w(F^2 > 3\sigma(F^2))$ |
| Pressure = 1.5 ± 0.5 kbar | |
| $a = 9.181(2)$ Å | space group: monoclinic $P2_1/a$ (No. 14) |
| $b = 12.350(1)$ Å | $T = 295$ K |
| $c = 6.267(3)$ Å | $\lambda = 0.710\ 73$ Å |
| $\beta = 106.11(2)°$ | $V = 682.7(3)$ Å$^3$ |
| $Z = 2$ | |
| $R(F_o) = 15.7$ | $R_w(F_o) = 5.3$ |
| $R(F^2 > 3\sigma(F^2)) = 4.9$ | $R_w(F^2 > 3\sigma(F^2)) = 4.2$ |
| Pressure = 3 ± 0.5 kbar | |
| $a = 9.147(1)$ Å | space group: monoclinic $P2_1/a$ (No. 14) |
| $b = 12.303(1)$ Å | $T = 295$ K |
| $c = 6.259(2)$ Å | $\lambda = 0.710\ 73$ Å |
| $\beta = 106.16(1)°$ | $V = 676.6(2)$ Å$^3$ |
| $Z = 2$ | |
| $R(F_o^2) = 16.3$ | $R_w(F_o^2) = 5.3$ |
| $R(F^2 > 3\sigma(F^2)) = 5.0$ | $R_w(F^2 > 3\sigma(F^2)) = 4.1$ |

[a] $R = \sum|F_o - F_c|/\sum|F_o|$. $R_w = [\sum w(F_o - F_c)^2/\sum F_o^2]^{1/2}$.

The powder measurements on $(NH_4)_2[Cu(H_2O)_6](SO_4)_2$ and $K_2[Cu(H_2O)_6](SO_4)_2$ were performed using a lever pressure cell of the type described by Weir *et al.*[19] The diffraction patterns were obtained using the Debye−Scherrer film technique (Mo $K\alpha_1$ radiation, bent Johansson monochromator). The powder reflections were indexed according to the JCPDS[20] diffraction pattern at ambient pressure, followed by the refinement of the unit cell parameters with the PARAM[21] computer program.

The unit cell parameters displayed in Figure 1 may be subject to small systematic errors, because they were measured in specific pressure cells. Thus, only the pressure dependencies of these parameters are significant and not the absolute magnitudes. In order to have correct reference values we independently determined the lattice constants of powder samples of $(NH_4)_2[Cu(H_2O)_6](SO_4)_2$ and $(ND_4)_2[Cu(D_2O)_6](SO_4)_2$ by calibrated high resolution X-ray diffractometry at 295 K and 1 bar, and the following parameters were obtained, respectively: $a = 9.200(1)$ Å, $b = 12.360(3)$ Å, $c = 6.296(1)$ Å, $\beta = 106.16(1)°$; $a = 9.299(2)$ Å, $b = 12.521(3)$ Å, $c = 6.204(1)$ Å, $\beta = 106.39\ (2)°$.

**1.3. Neutron Diffraction Measurements.** A single crystal of $K_2[Cu(H_2O)_6](SO_4)_2$ was immersed in the fluorinated hydrocarbon Fluorinert (3M Company) in a helium gas pressure cell mounted on the cold stage of a Displex closed-cycle helium refrigerator. (Air Products and Chemicals, Model CS-202). The sample was pressurized to 1.4 kbar and then cooled to 15 K. Time-of-flight neutron data were collected at the Intense Pulsed Neutron Source (IPNS) at Argonne National Laboratory using the single crystal diffractometer[21] equipped

(12) Simmons, C. J.; Hitchman, M. A.; Stratemeier, H.; Schultz, A. J. *J. Am. Chem. Soc.* **1993**, *115*, 11304.
(13) Robinson, D. J.; Kennard, C. H. L. *Cryst. Struct. Commun.* **1972**, *1*, 185.
(14) Whitnall, D. J.; Kennard, C. H. L.; Nimmo, J. K.; Moore, F. H. *Cryst. Struct. Commun.* **1975**, *4*, 702.
(15) Hitchman, M. A.; Waite, T. D. *Inorg. Chem.* **1976**, *15*, 2150.
(16) Merrill, L.; Bassett, W. A. *Rev. Sci Instrum.* **1974**, *45*, 290.
(17) Hazen, R. M.; Finger, L. W. *Rev. Sci Instrum.* **1981**, *52*, 75.
(18) Barnett, J. D.; Block, S.; Piermarini, G. *Rev. Sci Instrum.* **1973**, *44*, 1.
(19) Weir, C. E.; Block, S.; Piermarini, G. *J. Res. Natl. Bur. Stand.* **1965**, *69C*, 275.
(20) JPDS, Powder diffraction file No. 11-660 and 35-769.
(21) Schultz, A. J.; Srinivassen, K.; Teller, R. G.; Lukehart, C. M. *J. Am. Chem. Soc.* **1984**, *106*, 999. Schultz, A. J. *Trans. Am. Crystallogr. Assoc.* **1987**, *23*, 61.

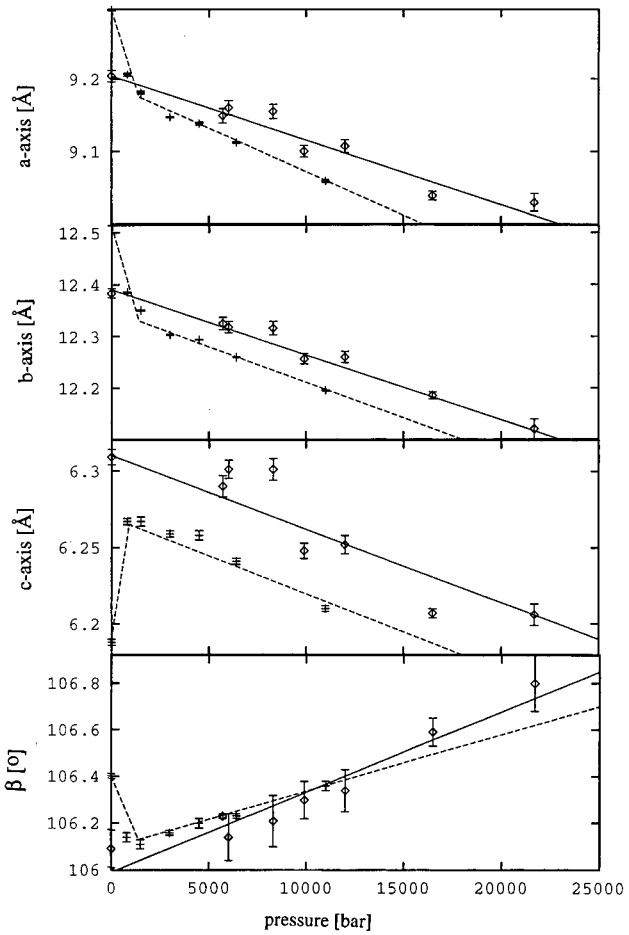


**Figure 1.** Unit cell parameters of $(ND_4)_2[Cu(D_2O)_6](SO_4)_2$ (dashed lines) and $(NH_4)_2[Cu(H_2O)_6](SO_4)_2$ (solid line) as a function of pressure (293 K).

**Table 2.** Unit Cell, Data Collection, and Refinement Parameters for $K_2Cu(SO_4)_2 \cdot 6H_2O$ at 15 K and 1.4 kbar

| | |
|---|---|
| space group | monoclinic $P2_1/a$ |
| $Z$ | 2 formula per unit cell |
| $a$ (Å) | 9.030(2) |
| $b$ (Å) | 12.022(3) |
| $c$ (Å) | 6.121(2) |
| $\beta$ (deg) | 104.29(3) |
| $V$ (Å$^3$) | 638.16(4) |
| radiation | neutrons |
| wavelength range | $\lambda = 0.7-4.2$ Å determined by time-of-flight |
| linear abs coeff $\mu$ (cm$^{-1}$) | $1.328 + 1.004\,\lambda$ |
| spherical abs cor radius $r$ (cm) | 0.1 |
| extinction param g (rad$^{-1} \times 10^{-4}$) | 0.042(3) |
| no. of reflcns in final ls ($F^2 > 3\,\sigma$) | 2508 |
| no. of unique reflcns | 1645 |
| function minimized | $\sum w(\|F_o\| - \|F_c\|)^2$ |
| $R(F)$ | 0.074 |
| $R^w(F)$ | 0.049 |
| GOF‘ | 1.061 |

with a position sensitive $^6$Li-glass scintillation detector.[22] Details of the data collection and analysis procedures have been previously provided.[23] Table 2 contains a summary of the data collection, analysis, and refinement parameters for the experiment.

An orientation matrix was initially obtained by an auto-indexing procedure[24] using data obtained by searching a histogram for peaks. The 120 time-of-flight histogram channels were constructed with constant $\Delta t/t = 0.015$ and correspond to wavelengths of 0.7−4.2 Å. Bragg reflections were integrated about their predicted location and were corrected for the Lorentz factor, the incident spectrum, the detector efficiency and dead-time losses. A wavelength-dependent spherical absorption correction was applied.[25] Symmetry-related reflections were not averaged since different extinction factors were applicable to reflections measured at different wavelengths. Atomic scattering lengths used in the least-squares refinements were those tabulated by Sears.[26] In the final cycles of least-squares refinements, all atoms were treated with anisotropic temperature factors and a secondary extinction correction (Becker and Coppens formalism,[27] Type I, Lorentzian distribution) was included. Table 7 gives the final atomic coordinates and isotropic temperature factors. Interatomic distances and angles are given in Table 8. Anisotropic temperature factors and observed and calculated structure factors are given as supplementary material.

**1.4. EPR Measurements over a Pressure Range.** The EPR spectra were measured using a custom built spectrometer operating at Q-band frequency (∼35 GHz) with a modulation frequency of 30 Hz. To vary the pressure, the powdered samples were placed in a chamber of nonmagnetic beryllium bronze filled with dry oil as the pressure-transmitting medium, as described in detail elsewhere.[28] The pressure was determined by measuring the resistance of a coil of manganin wire, the uncertainty being estimated as 0.05 kbar.

## 2. Results and Discussion

**2.1. Crystal Structure of $(ND_4)_2[Cu(D_2O)_6](SO_4)_2$.** The structure of $(ND_4)_2[Cu(D_2O)_6](SO_4)_2$, determined by X-ray diffraction, was solved at pressures of 1 bar, ∼1.5 kbar, and ∼3.0 kbar using isotropic temperature factors utilizing the program XLS of the ShelXTL Plus system,[29] taking as the starting point for the refinement the unit cell parameters and atomic coordinates previously reported for this compound by Hathaway and Hewat.[11] In each case, solution of the structure proceeded smoothly, leading to weighted $R_w(F^2 > 3\sigma(F^2))$ factors of 3.9, 4.2, and 4.1% for the three pressures, respectively. The deuterium atoms were not included in the refinement. The atomic coordinates and isotropic temperature factors are listed in Table 3.

The unit cell parameters of the high and low pressure forms of $(ND_4)_2[Cu(D_2O)_6](SO_4)_2$ differ significantly, and plots of these obtained by powder X-ray diffraction over the pressure range 1 bar to 22 kbar are shown in Figure 1, together with the values observed for the corresponding hydrogenous compound. For the latter, the three unit cell lengths decrease gradually with increase in pressure, as expected, and the monoclinic angle increases slightly. For the deuterated compound, the $a$ and $b$ axes and the angle $\beta$ all decrease between 1 bar and ∼1.5 kbar, during which the compound alters structure, while the $c$ axis *increases* significantly. At 1.5 kbar and above, all four cell parameters behave in a manner similar to those of the hydrogenous compound. Upon returning to 1 bar pressure, the unit cell parameters revert to those observed prior to the pressure increase, indicating that the structural change is reversible.

The most important concern of the present study is the geometry of the $Cu(D_2O)_6^{2+}$ group. This is centrosymmetric, and the three Cu−O distances at 1 bar pressure are listed in Table 4. They are similar to those reported previously[11] on the basis of a powder neutron diffraction determination. The bond

(22) Schultz, A. J. *Trans. Am. Crystallogr. Assoc.* **1993**, *29*, 29.
(23) Schultz, A. J.; Van Derveer, D. G.; Parker, D. W.; Balwin, J. E. *Acta Crystallogr., C* **1990**, *46*, 276.
(24) Jacobson, R. A. *J. Appl. Crystallogr.* **1986**, *19*, 283.
(25) Howard, J. A.; Johnson, O.; Schultz, A. J.; Stringer, A. M. *J. Appl. Crystallogr.* **1987**, *20*, 120.
(26) Sears, V. F. Methods of Experimental Physics 23; *Neutron Scattering, Part A*; Sköld, K., Price, D. L., Eds.; Academic Press: Orlando, FL, 1986; pp 521−550.
(27) Becker, P. J.; Coppens, P. *Acta Crystallogr., A* **1974**, *30*, 129.
(28) Kozhukhar, A. Yu.; Lukin, S. N.; Tsintsandze, G. A.; Shapolavov, V. A. *Prib. Tekh. Eksp.* **1975**, *4*, 198 (*Cryogenics* **1976**, 441).
(29) Sheldrick, G. M. ShelXTL Plus™ 4.0 Computer program. Siemens Analytical X-ray Instruments Inc., 1990.

**Table 3.** Atomic Coordinates and Isotropic Temperature Factors[a] for $(ND_4)_2Cu(SO_4)_2 \cdot 6D_2O$ (293 K)[b]

| atom | *x* | *y* | *z* | *B* (Å$^2$) |
|---|---|---|---|---|
| Cu1 | 0 | 0 | 0 | 1.7(1) |
| | 0 | 0 | 0 | 1.6(1) |
| | 0 | 0 | 0 | 1.6(1) |
| S2 | 0.3963(3) | 0.1418(2) | 0.7502(14) | 2.0(1) |
| | 0.4093(3) | 0.1393(2) | 0.7513(13) | 1.9(1) |
| | 0.4111(3) | 0.1384(2) | 0.7494(13) | 1.8(1) |
| O3 | 0.3927(7) | 0.2358(5) | 0.6017(26) | 2.4(2) |
| | 0.4133(7) | 0.2312(5) | 0.5980(27) | 2.8(2) |
| | 0.4176(7) | 0.2299(6) | 0.5974(28) | 2.7(2) |
| O4 | 0.5384(7) | 0.0812(5) | 0.7672(28) | 2.4(2) |
| | 0.5492(7) | 0.0746(5) | 0.7724(27) | 2.6(2) |
| | 0.5508(8) | 0.0718(5) | 0.7722(28) | 2.6(2) |
| O5 | 0.2673(7) | 0.0716(5) | 0.6297(25) | 2.3(2) |
| | 0.2782(7) | 0.0694(5) | 0.6351(26) | 2.2(2) |
| | 0.2769(7) | 0.0691(5) | 0.6312(26) | 2.0(2) |
| O6 | 0.3755(9) | 0.1776(6) | 0.9725(35) | 3.2(2) |
| | 0.3857(8) | 0.1818(6) | 0.9600(36) | 2.3(2) |
| | 0.3861(9) | 0.1819(6) | 0.9612(38) | 3.0(2) |
| O7 | 0.1621(7) | 0.1097(5) | 0.1673(28) | 2.7(2) |
| | 0.1775(7) | 0.1150(5) | 0.1832(29) | 2.7(2) |
| | 0.1800(7) | 0.1153(5) | 0.1840(30) | 2.7(2) |
| O8 | −0.1786(8) | 0.1140(5) | 0.0423(27) | 2.6(2) |
| | −0.1656(7) | 0.1110(5) | 0.0355(26) | 2.1(2) |
| | −0.1649(7) | 0.1109(5) | 0.0364(26) | 1.9(2) |
| O9 | 0.0006(7) | −0.0647(5) | 0.2837(26) | 2.1(2) |
| | −0.0034(7) | −0.0646(5) | 0.2785(27) | 2.0(2) |
| | −0.0041(7) | −0.0637(5) | 0.2818(29) | 2.2(2) |
| N10 | 0.1252(9) | 0.3560(6) | 0.3748(31) | 2.4(2) |
| | 0.1323(8) | 0.3477(6) | 0.3659(31) | 2.0(2) |
| | 0.1340(8) | 0.3458(6) | 0.3674(32) | 2.0(2) |

[a] temperature factors defined by: $f' = f \exp(-B(\sin^2\theta)/\lambda^2)$. [b] Rows 1, 2, and 3 refer to pressures 1 bar, 1.5 kbar, and 3 kbar, respectively.

**Table 4.** Cu−O Bond Lengths (Å) in $(ND_4)_2Cu(SO_4)_2 \cdot 6D_2O$ at Different Pressures and Temperatures

| | 1 bar | 1 bar | 1 bar, 15 K | 1.5 kbar | 1.5 kbar, 15 K | 3.0 kbar |
|---|---|---|---|---|---|---|
| Cu−O7 | 2.085(7) | 2.081(6) | 2.022(2) | 2.225(8) | 2.290(2) | 2.235(8) |
| Cu−O8 | 2.260(8) | 2.242(7) | 2.310(2) | 2.104(8) | 2.014(2) | 2.093(8) |
| Cu−O9 | 1.932(15) | 1.927(6) | 1.966(3) | 1.927(16) | 1.988(3) | 1.940(17) |
| ref | this work | 11 | 12 | this work | 12 | this work |

distances measured previously by neutron diffraction at 15 K and 1 bar and 1.5 kbar pressure[12] are also given in Table 4 for comparison. At 295 K and 1 bar pressure, the $Cu(D_2O)_6^{2+}$ group has an orthorhombic geometry, with the Cu−O7 distance almost midway between the short bond to O9, and the long bond to O8. At a pressure of ∼1.5 kbar, although the lengths of the intermediate and long Cu−O bonds do not change markedly, their directions switch, with the long bonds now occurring to O7 rather than O8, and this pattern is maintained at ∼3.0 kbar. The basic structure of the compound is illustrated in Figure 2. An important feature of the structural change under external pressure involves motion of the sulfate ion with respect to the $Cu^{2+}$, and a rotation of this group around the S2−O5 axis. These displacements ensure that—though the Cu−O7 and Cu−O8 bonds switch in length—the hydrogen bonds between the O7, O8, and O9 atoms coordinated to $Cu^{2+}$ and the oxygen atoms of the sulfate ion (Figure 2) remain practically unchanged (Table 5). The only significant change in the hydrogen bonding network in the high pressure structure, is that the N−O4 hydrogen bond is weakened, while in compensation the N−O3 hydrogen bond involving the D(13) atom (Figure 2) is considerably shortened (Table 5). This effect was noted previously in the comparison of the high and low pressure structures measured at 15 K.[12] It is apparent that both alternative structures are

**Table 5.** Hydrogen (Deuterium) Bonds (Å) in $(ND_4)_2Cu(SO_4)_2 \cdot 6D_2O$ (295 K) at Different Pressures

| | 1bar | 1.5 kbar | 3 kbar |
|---|---|---|---|
| N−O6 | 2.92(2) | 2.92(2) | 2.92(2) |
| N−O3 (D12) | 2.91(1) | 2.96(1) | 2.96(1) |
| N−O3 (D13) | 3.11(2) | 2.96(2) | 2.91(2) |
| N−O4 | 2.88(3) | 3.01(2) | 3.02(3) |
| N−O5 | 2.88(1) | 2.86(1) | 2.87(1) |
| O7−O5 | 2.79(2) | 2.78(2) | 2.75(2) |
| O7−O6 | 2.73(2) | 2.79(2) | 2.76(2) |
| O8−O4 | 2.73(1) | 2.72(1) | 2.71(1) |
| O8−O6 | 2.71(1) | 2.67(1) | 2.66(1) |
| O9−O5 | 2.69(1) | 2.72(1) | 2.70(1) |
| O9−O3 | 2.71(1) | 2.70(1) | 2.70(1) |

stabilized by very similar hydrogen bonding networks. As might be expected, the overall packing in the high pressure phase (**H**) is somewhat denser than that in the low pressure form (**L**), the unit cell parameters implying a decrease in volume of ∼0.4% (Figure 1). The expansion of the *c* axis at high pressure is due to the fact that neighboring $Cu(D_2O)_6^{2+}$ complexes are connected via the hydrogen bonding linkage: O7−D15−O5−D19−O9. As the Cu−O7 bond becomes longer at high pressure and the lengths of the hydrogen bonds in this linkage remain roughly constant, the Cu−Cu distance defining the *c* axis increases.

The data collected in Table 6 suggest that it is generally possible to distinguish between two alternative structural types not only for the Jahn−Teller cations $Cu^{2+}$ and $Cr^{2+}$, but even for cations such as $Ni^{2+}$ and $Zn^{2+}$, using criteria such as the positional parameter *x* of the sulfur atom, the *a*/*c* ratio, and the N−D13−O3 and N−D13−O4 hydrogen bond distances. For the **L** modification, M−O8 > M−O7, *x* and *a*/*c* are lower than 0.405 and larger than 1.5, respectively, and the N−O3 hydrogen bond is distinctly longer than that between the nitrogen and O4. For most ammonium Tutton salts the reverse is true, and the characteristics of the **H** modification are shown (Table 6).

The structural change between 1 bar and ∼1.5 kbar is broadly similar to that observed previously at 15 K,[12] as may be clearly seen from the Cu−O bond distances listed in Table 4. However, at 15 K the bond lengths in the $CuO_6$ group approximate much more closely to the tetragonally elongated octahedral coordination geometry commonly observed for copper(II) complexes than is the case at 295 K. It has been suggested[11,12] that this is because two structural forms of the $Cu(D_2O)_6^{2+}$ group, with bond lengths similar to those in the **L** and **H** modifications at low temperature, are in thermal equilibrium. This means that while the low temperature structure reveals the true local coordination geometry about the Cu, at higher temperatures the crystal structures show the *average* positions for the two geometries, weighted by their thermal population. This behavior is reminiscent of that originally observed by Silver and Getz[7] in a study of the temperature dependence of the EPR spectrum of the $Cu(H_2O)_6^{2+}$ ion in $Cu^{2+}$-doped $K_2[Zn(H_2O)_6](SO_4)_2$. The data were interpreted using a model which has subsequently been applied to the EPR spectra[1,8] and X-ray crystal structures[1,10] of a range of "dynamic" copper(II) complexes.

The Silver and Getz approach assumes identical geometries for the complexes involved in the equilibrium, which differ solely in their energy and orientation in the crystal lattice. At 15 K, the bond lengths of the $Cu(D_2O)_6^{2+}$ ion in the **L** and **H** phases of $(ND_4)_2[Cu(D_2O)_6](SO_4)_2$ are similar (Table 4), and this prompted the suggestion[12] that these basically represent the groups involved in the thermal equilibrium responsible for the structural change observed at higher temperature. The effect of pressure is then to change the lattice "strain" acting on the $Cu(D_2O)_2^{2+}$ complex, and hence the relative energy of the two

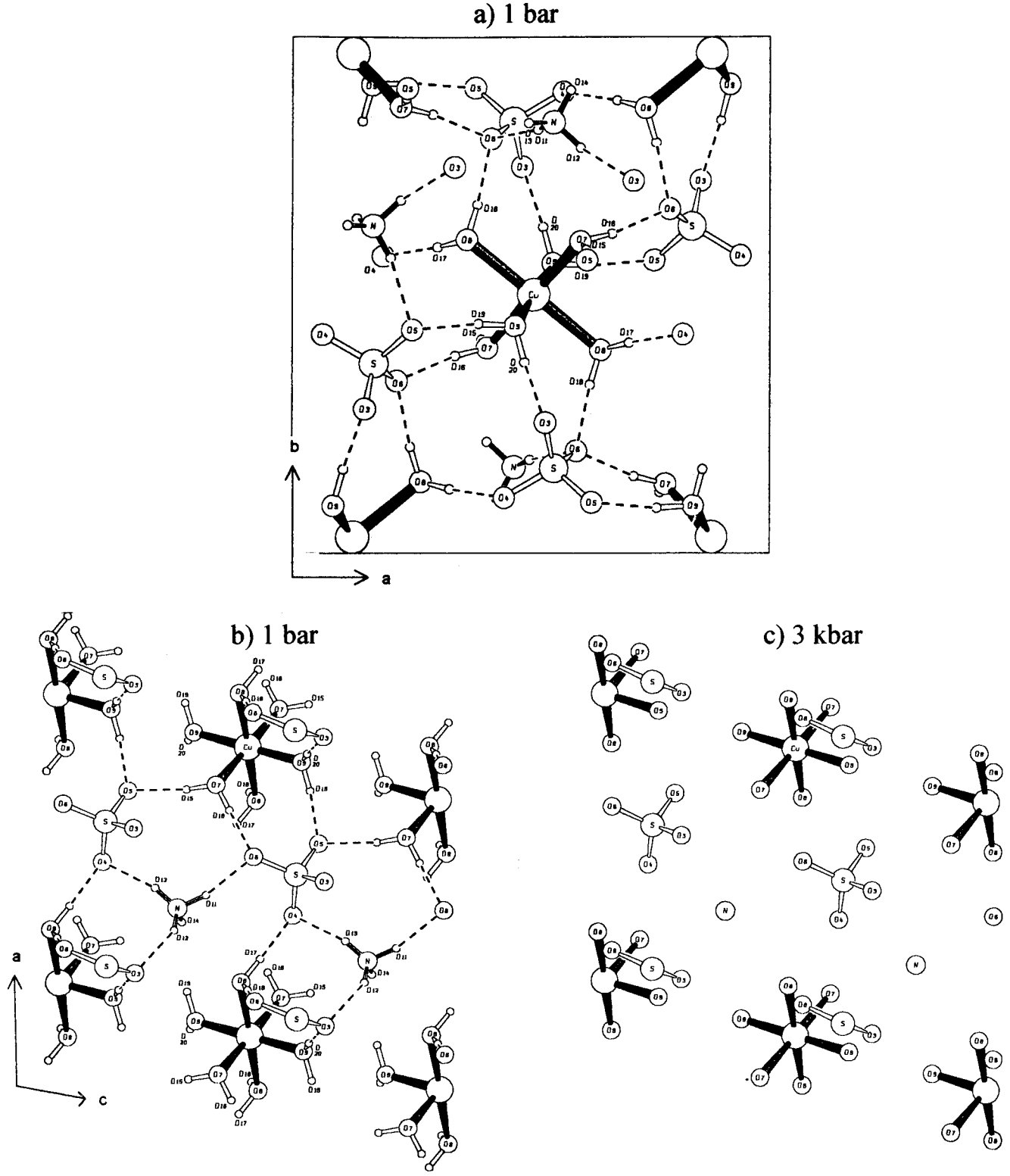


**Figure 2.** Structure of $(ND_4)_2[Cu(D_2O)_6](SO_4)_2$ at 295 K and 1 bar, viewed perpendicular to the *ab* plane (a) and down the crystallographic *b* direction (b). The important hydrogen bridges are marked with D atom positions adapted from ref 11. The structure at ~3 kbar and 295 K viewed along *b* is depicted in part c. This projection—in comparison to part b— shows the switch between the Cu−O7 and Cu−O8 spacings.

forms, with the ground state switching between 1 bar and 1 kbar. To a first approximation, it is just the Cu−O7 and Cu−O8 bond lengths which are involved in the equilibrium. However, it must be noted that the two phases differ not only in this aspect, but also in other structural features discussed above; moreover, the geometry of the $Cu(D_2O)_6^{2+}$ ion has a smaller orthorhombic distortion in the **H** modification. The potential surface of the complex in the two phases is illustrated in Figure 3, together with schematic diagrams illustrating the bonds involved in the equilibrium (the potential surfaces are described in greater detail in ref 12).

Assuming that the Silver−Getz model holds to a reasonable approximation, namely, that the molecular geometry is independent of temperature and the higher energy conformer differs from that at low energy simply by interchange of the above bond lengths, then the fraction *x* of the complexes in the higher

**Table 6.** Geometric Parameters for Various Tutton Salts, Characterizing the Two Possible Structural Modifications

| | | Cu−O7 (Å) | Cu−O8 (Å) | Cu−O9 (Å) | N−(D13)−O3 (Å) | N−(D13)−O4 (Å) | *x*-positional param for S | a/c | ref |
|---|---|---|---|---|---|---|---|---|---|
| 1 | $(ND_4)_2[Cu(D_2O)_6](SO_4)_2$ at 295 K | 2.085(7) | 2.260(8) | 1.932(15) | 3.11 | 2.88 | 0.3963(3) | 1.502 | this work |
| 2 | $(ND_4)_2[Cu(D_2O)_6](SO_4)_2$ at 295 K and 1.5 kbar | 2.225(8) | 2.104(8) | 1.927(16) | 2.96 | 3.01 | 0.4093(3) | 1.465 | this work |
| 3 | $(ND_4)_2[Cu(D_2O)_6](SO_4)_2$ at 295 K and 3 kbar | 2.235(8) | 2.093(8) | 1.940(17) | 2.91 | 3.02 | 0.4111(3) | 1.461 | this work |
| 4 | $(NH_4)_2[Cu(H_2O)_6](SO_4)_2$ at 298 K | 2.216(1) | 2.078(1) | 1.962(1) | 3.01 | 3.12 | 0.4101(3) | 1.463 | 30 |
| 5 | $(NH_4)_2[Zn(H_2O)_6](SO_4)_2$ at 295 K | 2.109(1) | 2.106(1) | 2.062(1) | 2.99 | 3.14 | 0.4075(1) | 1.478 | 31 |
| 6 | $(ND_4)_2[Zn(D_2O)_6](SO_4)_2$ at 295 K | 2.107(3) | 2.105(3) | 2.062(3) | 3.00 | 3.17 | 0.4073(1) | 1.477 | 32 |
| 7 | $(NH_4)_2[Ni(H_2O)_6](SO_4)_2$ at 295 K | 2.068(1) | 2.066(1) | 2.037(1) | 2.88[a] | 3.23[a] | 0.4078(3) | 1.471 | 33 |
| 8 | $(ND_4)_2[Ni(D_2O)_6](SO_4)_2$ at 2 K | 2.066(3) | 2.062(3) | 2.038(3) | 2.87 | 3.22 | 0.4128(3) | 1.451 | 34 |
| 9 | $(NH_4)_2[Mg(H_2O)_6](SO_4)_2$ at 295 K | 2.073(5) | 2.083(5) | 2.051(5) | 3.06 | 3.10 | 0.4047(2) | 1.501 | 35 |
| 10 | $(NH_4)_2[Cr(H_2O)_6](SO_4)_2$ at 295 K | 2.125(2) | 2.323(2) | 2.054(1) | 3.32 | 2.89 | 0.3965(1) | 1.519 | 36 |

[a] At 2 K.[30]

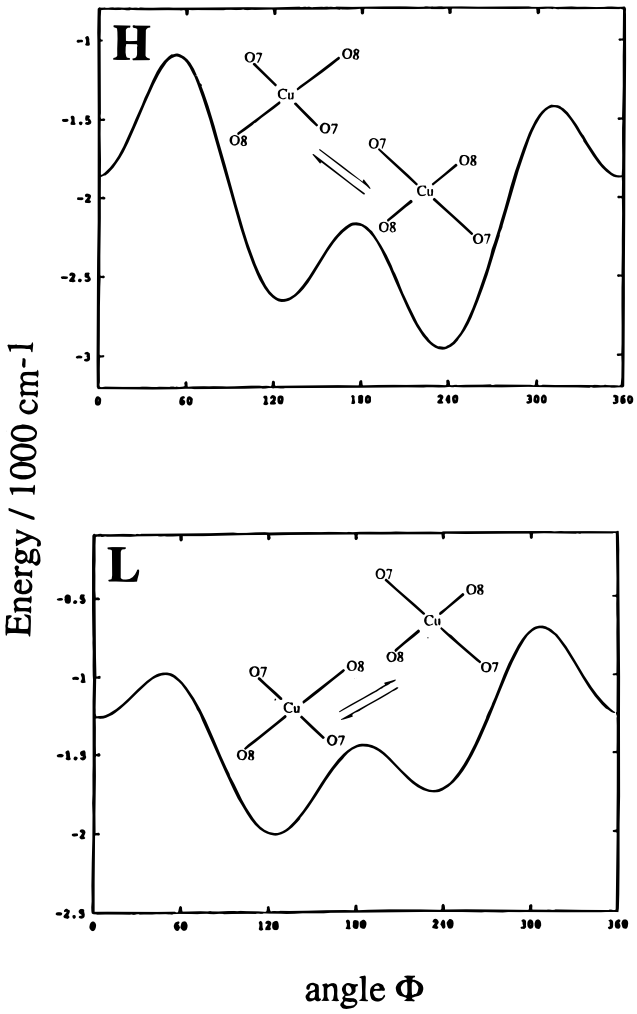


**Figure 3.** Ground state potential surface of the $Cu(D_2O)_6^{2+}$ complex in the high pressure (**H**) and low pressure (**L**) phases of $(ND_4)_2[Cu(D_2O)_6](SO_4)_2$. The difference in the geometrical conformers associated with the lowest vibronic level in each well are illustrated schematically (see ref 12 for the parameters used to define the potential surfaces).

energy state may be obtained independently from the following expressions:

$$(1 - x)R[O7]_{15\,K} + xR[O8]_{15\,K} = R[O7]_{295\,K} \qquad (1)$$

$$(1 - x)R[O8]_{15\,K} + xR[O7]_{15\,K} = R[O8]_{295\,K} \qquad (2)$$

Here, $R$ is the bond length to the atom in brackets at the temperature given by the subscript. The Cu−O7 distance (eq 1) suggests that in the **L** phase at 295 K ∼22% of the $Cu(D_2O)_6^{2+}$ ions are in the higher energy state (that with the longer bonds to O7), while the Cu−O8 distance (eq 2) implies that ∼17% are in this state. The good agreement between the estimates suggests that the model is realistic. For the **H** phase at 1.5 kbar the calculated values at 295 K are 28% and 30%, while at ∼3.0 kbar the estimates are 25% and 26%.

In summary, the low and high pressure phases of $(ND_4)_2[Cu(D_2O)_6](SO_4)_2$ both undergo a thermal equilibrium involving a higher energy state in which the $Cu(D_2O)_6^{2+}$ ions adopt a geometry similar to that of the alternative conformation, with a broadly similar proportion being in the upper state at 295 K for both phases. While there appears to be some change in stucture between ∼1.5 and ∼3.0 kbar, this is quite modest, and for the high pressure phase the position of the thermally induced equilibrium is therefore rather insensitive to pressure. The two phases of $(ND_4)_2[Cu(D_2O)_6](SO_4)_2$ have identical space groups, and the EPR suggests that the relative energies of the two orientations of the $Cu(D_2O)_6^{2+}$ group change smoothly and progressively as the pressure-induced phase change occurs (see section 2.3). Since the relative energies of the two conformations depend upon the interactions with the surrounding lattice, it seems likely that the change from the **L** to **H** phase occurs gradually as the pressure is raised from 1 bar to 1.5 kbar for the lattice as a whole. This suggests that the transition is second order, though the change ocurs over a rather narrow pressure range. At low temperature, when thermal population of the higher energy levels is negligible, the phase change is expected to occur over a very narrow pressure change.

**2.2. Crystal Structure of $K_2[Cu(H_2O)_6](SO_4)_2$.** An X-ray structure determination at 295 K has shown[13] that the disposition of the Cu−O bonds in the potassium Tutton salt is similar to that in $(ND_4)_2[Cu(D_2O)_6](SO_4)_2$, so that it is of interest to see whether this shows a switch in structure at high pressure, similar to that observed for the deuterated ammonium salt. In this context it is interesting to note that such a switch does indeed occur at 1 bar pressure when the sulfate anions are replaced by selenate.[14] The structure of a single crystal of $K_2[Cu(H_2O)_6](SO_4)_2$ was determined at 15 K and 1.4 kbar pressure by time-of-flight neutron diffraction. The refinement of the structure proceeded smoothly to an $R(F^2 > 3\sigma(F^2))$ factor of 7.4% and weighted $R_w(F^2 > 3\sigma(F^2))$ factor of 4.9%, taking the unit cell parameters and atomic coordinates of the previous structure as the starting point of the refinement. Atomic coordinates and thermal parameters are listed in Table 7, and bond distances and angles in Table 8. The coordination geometry about the copper is broadly similar to that observed at 295 K in the previous X-ray study,[13] where Cu−O7 = 2.069(2) Å, Cu−O8 = 2.278(2) Å, Cu−O9 = 1.943(2) Å. Up to 1.4 kbar, $K_2[Cu(H_2O)_6](SO_4)_2$ thus undergoes no switch in Cu−O bond lengths like that observed for $(ND_4)_2[Cu(D_2O)_6](SO_4)_2$ with increasing pressure. The dependence of the unit cell parameters upon pressure (Figure 4) suggests that this is the case up to a pressure of 42 kbar, as no discontinuities similar to those exhibited by

**Table 7.** Atomic Positional and Equivalent Isotropic Thermal Parameters for $K_2[Cu(H_2O)_6](SO_4)_2$ at 15 K and 1.4 kbar from Neutron Diffraction Data

| atom | *x* | *y* | *z* | $U_{eq}$ (Å$^2$)[a] |
|---|---|---|---|---|
| Cu1 | 0.0 | 0.0 | 0.0 | 0.0045(4) |
| S2 | 0.4012(3) | 0.1316(2) | 0.7178(4) | 0.0043(7) |
| O3 | 0.3972(2) | 0.2334(1) | 0.5772(2) | 0.0075(4) |
| O4 | 0.5456(1) | 0.0716(1) | 0.7349(2) | 0.0081(4) |
| O5 | 0.2716(1) | 0.0592(1) | 0.6062(2) | 0.0072(4) |
| O6 | 0.3859(1) | 0.1642(1) | 0.9453(2) | 0.0075(4) |
| O7 | 0.1609(2) | 0.1103(1) | 0.1612(2) | 0.0078(4) |
| O8 | −0.1903(2) | 0.1219(1) | 0.0389(2) | 0.0082(4) |
| O9 | −0.0018(1) | −0.0648(1) | 0.2899(2) | 0.0068(3) |
| K | 0.1221(2) | 0.3436(2) | 0.3421(4) | 0.0069(6) |
| H15 | 0.2083(3) | 0.0859(2) | 0.3164(5) | 0.0203(8) |
| H16 | 0.2437(3) | 0.1215(2) | 0.0853(5) | 0.0217(8) |
| H17 | −0.2844(3) | 0.1038(2) | −0.0731(5) | 0.0213(8) |
| H18 | −0.1624(3) | 0.1966(2) | −0.0003(5) | 0.0217(9) |
| H19 | −0.1002(3) | −0.0575(2) | 0.3321(5) | 0.0205(8) |
| H20 | 0.0340(3) | −0.1429(2) | 0.3238(5) | 0.0198(8) |

[a] Atom refined anisotropically, where $U_{eq} = {}^1/_3\sum_{ij}U_{ij}a_i^*a_j^*\mathbf{a}_i\cdot\mathbf{a}_j$.

**Table 8.** Bond Lengths and Angles for $K_2Cu(SO_4)_2\cdot 6H_2O$ at 1.4 kbar and 15 K

| | | | |
|---|---|---|---|
| | Bond Lengths (Å) | | |
| Cu1−O7 | 2.034(2) | O7−H15 | 0.985(3) |
| Cu1−O8 | 2.316(1) | O7−H16 | 0.982(3) |
| Cu1−O9 | 1.942(1) | O8−H17 | 0.976(4) |
| S2−O3 | 1.491(3) | O8−H18 | 0.978(3) |
| S2−O4 | 1.471(3) | O9−H19 | 0.989(3) |
| S2−O5 | 1.484(3) | | 0.998(3) |
| S2−O6 | 1.486(3) | | |
| | H bonds less than 1.8 Å | | |
| O3−H20 | 1.667(3) | O5−H15 | 1.754(3) |
| O4−H17 | 1.731(4) | O6−H18 | 1.781(3) |
| O5−H19 | 1.681(3) | O6−H16 | 1.786(3) |
| | Bond Angles (deg) | | |
| O7−Cu1−O8 | 89.83(6) | O3−S2−O6 | 109.27(18) |
| O7−Cu1−O9 | 89.10(6) | O4−S2−O5 | 109.20(18) |
| O8−Cu1−O9 | 89.21(6) | O4−S2−O6 | 110.40(20) |
| O3−S2−O4 | 109.81(16) | O5−S2−O6 | 109.94(15) |
| O3−S2−O5 | 108.18(20) | | |

the deuterated ammonium compound occur. However, comparison of the Cu−O bond distances of $K_2[Cu(H_2O)_6](SO_4)_2$ at 15 K and 1.4 kbar (Table 8) with those at 295 K and 1 bar shows that while the Cu−O9 lengths are similar, the Cu−O7 is shorter and the Cu−O8 distance is significantly longer at the lower temperature. The difference is unlikely to be caused by the change in pressure, as this has no significant effect on the *g* values at 295 K (see following section), but again seems to be due to the thermal population of a higher energy state in which the lengths of these two bonds interchange at 295K. Substitution of the bond lengths in eqs 1 and 2 implies that ∼16% of the complexes are in the higher energy state at this temperature, a somewhat smaller proportion than that deduced for the analogous ammonium and deuterated ammonium salts. The pressure dependence of the unit cell parameters of $K_2[Cu(H_2O)_6](SO_4)_2$ (Figure 4) is very similar to that of the ammonium salt (Figure 1), though the structures are different. The respective gradients are nearly identical, indicating a homogeneous shrinking of the unit cell due to the applied pressure in both structures.

The unit cell of $K_2[Cu(H_2O)_6](SO_4)_2$ viewed down *c** is shown in Figure 5, and short hydrogen bonding distances are listed in Table 8. The hydrogen bonding interactions between the water molecules and sulfate groups are similar to those of the deuterated ammonium salt at ambient pressure (Table 5) which is consistent with the similar disposition of the metal complexes in the two unit cells. Unlike the deuterated ammonium compound, no hydrogen-bonding interactions involving the cations occur for the potassium salt, and this may possibly be one reason why this compound does not exhibit a high pressure structural form analogous to that of the former salt.

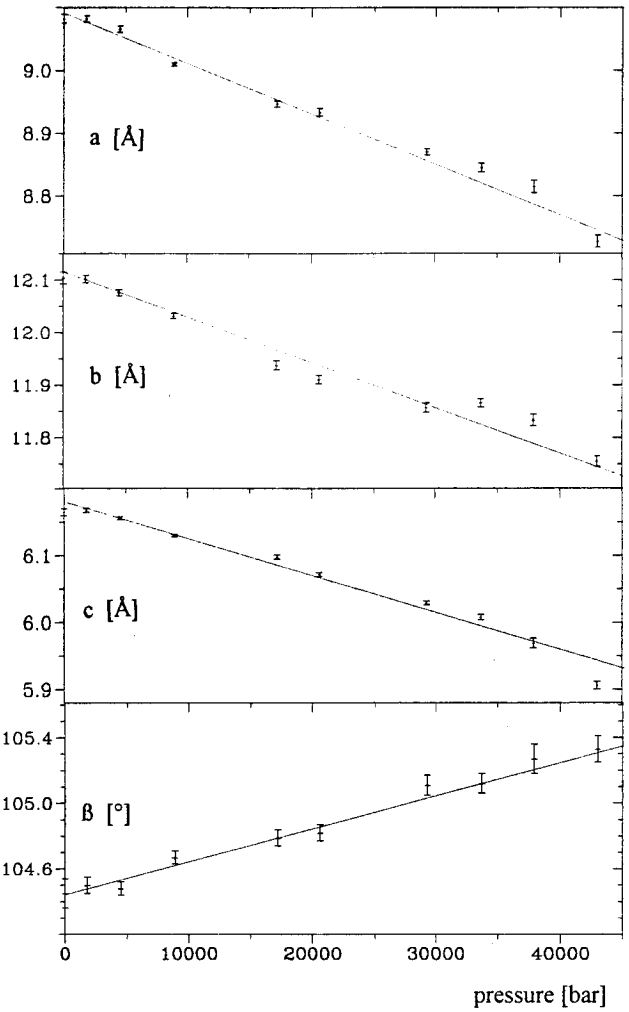


**Figure 4.** Dependence of the unit cell parameters of $K_2[Cu(H_2O)_6](SO_4)_2$ upon pressure at 295 K.

**2.3. Pressure Dependence of the EPR Spectrum of $(ND_4)_2[Cu(D_2O)_6](SO_4)_2$.** The Q-band EPR spectrum of powdered $(ND_4)_2[Cu(D_2O)_6](SO_4)_2$ was recorded at 303 K at various pressures between 1 bar and ∼10 kbar. Measurements were made at intervals of ∼0.2 kbar in the range 1 bar to 1 kbar, and of ∼2 kbar between 1 and 10 kbar. Representative spectra are shown in Figure 6a. Similar spectra were obtained irrespective of whether the pressure was increased or decreased *ie* there was no evidence for any "hysteresis" effects based on pressure changes of ∼0.2 kbar. The variation of the *g* values, estimated by simulating the spectra as a function of pressure is shown in Figure 7a. At 1 bar the spectrum is characteristic of an orthorhombic **g** tensor. On applying pressure, the peaks associated with the two larger *g* values coalesce and the spectrum at 0.52 kbar is typical of a **g** tensor of tetragonal symmetry with the symmetry axis associated with the smallest *g* value. On increasing the pressure further, an orthorhombic spectrum redevelops until at ∼1.5 kbar the final spectral shape is attained. It should be noted that the spectra at 1 bar and above 1.5 kbar are different, with a more pronounced orthorhombicity in the former case. This also occurs in the respective Cu−O distances at both 295 and 15 K at these pressures (Table 4), reflecting the different lattice interactions acting on the $Cu(D_2O)_6^{2+}$ groups in the two phases.

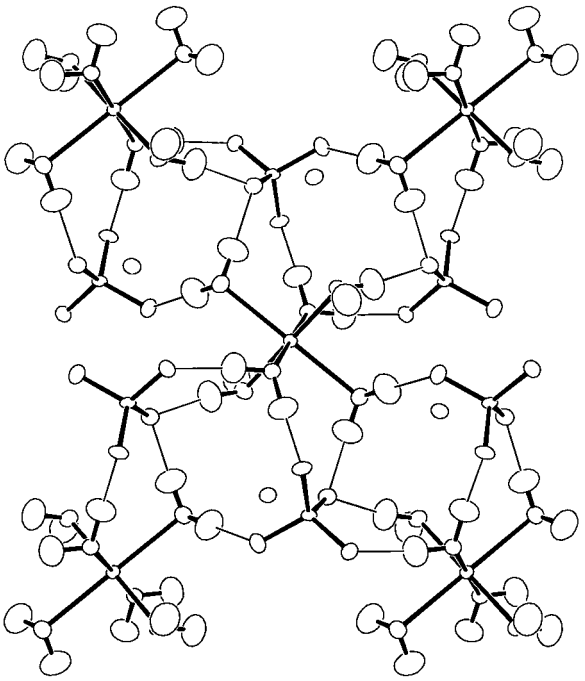

**Figure 5.** Unit cell of $K_2[Cu(H_2O)_6](SO_4)_2$ viewed down $c^*$ at 295 K. Numbering of the atoms is similar to that of the deuterated ammonium salt.

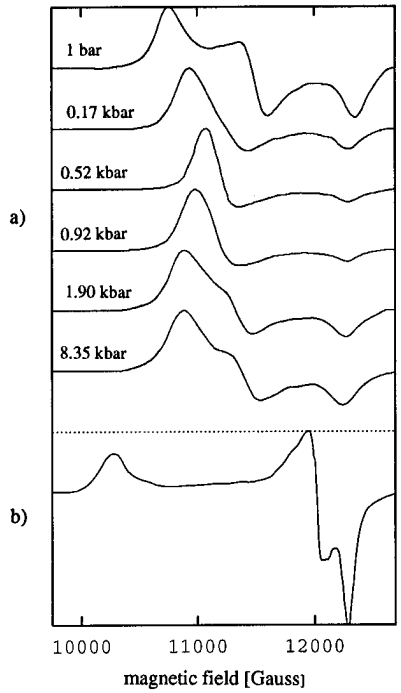


**Figure 6.** (a) EPR spectrum of powdered $(ND_4)_2[Cu(D_2O)_6](SO_4)_2$ at 303 K and various pressures. (b) EPR spectrum of powdered $(ND_4)_2[Cu(D_2O)_6](SO_4)_2$ at 77 K and 1 bar pressure.

The highly orthorhombic **g** tensor at 1 bar, $g_1 = 2.061$, $g_2 = 2.205$, and $g_3 = 2.350$, clearly conforms to the weighted average of the two structural conformers in thermal equilibrium, rather than to the "time-frozen" molecular geometry which has close to axial symmetry. The powder spectrum at 77 K and 1 bar pressure is shown in Figure 6b for comparison (a detailed study[15] suggests that this is the limiting spectrum reached at low temperature, so that it corresponds to the basic spectrum of the $Cu(D_2O)_6^{2+}$ complex in the **L** phase). Apparently at 303 K the rate of exchange between the forms, illustrated in Figure 3, must be more rapid than the energy difference between their

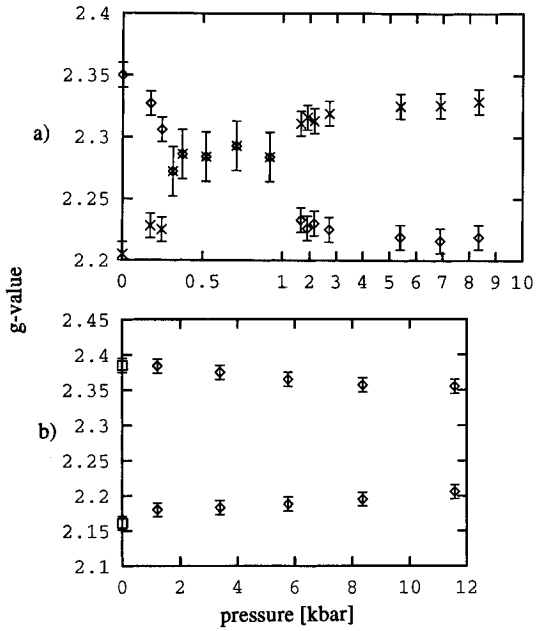


**Figure 7.** Variation of the two higher $g$ values as a function of pressure: (a) $(ND_4)_2[Cu(D_2O)_6](SO_4)_2$ at 303 K; (b) $K_2[Cu(H_2O)_6](SO_4)_2$ at 295 K.

EPR signals measured in frequency units, $\sim 10^9$ Hz.[37] The rate of electron exchange between *different* complexes in the unit cell is significantly slower than this, as signals corresponding to the two magnetically inequivalent molecules in the unit cell are resolved in EPR measurements on single crystals of $(ND_4)_2[Cu(D_2O)_6](SO_4)_2$.[15,38] Assuming that the structural isomers have similar $g$ values, but with the directions of the upper two $g$ values interchanged, the values associated with each bond direction are given by expressions exactly analogous to those (eqs 1 and 2) describing the bond lengths observed by X-ray diffraction:

$$(1 - x)g[O7]_{77\ K} + xg[O8]_{77\ K} = g[O7]_{303\ K} \qquad (3)$$

$$(1 - x)xg[O8]_{77\ K} + xg[O7]_{77\ K} = g[O8]_{303\ K} \qquad (4)$$

The molecular $g$ values at 77 K are $g(O7) = 2.117$, $g(O8) = 2.446$, and $g(O9) = 2.066$, with the directions being confirmed by measurements on a single crystal.[15,38] The close similarity of the lowest $g$ values at 77 K and 303 K is consistent with the fact that the Cu−O9 bond lengths are similar at 15 and 295 K (Table 4). Substitution of the appropriate values into eqs 3 and 4 implies thermal excitation of 28 ± 1% of the complexes into the higher state, a somewhat higher value than those obtained from the bond distances (22% and 17%, see section **2.1**). A spectrum measured at 295 K and 1 bar[38] yielded the $g$ values 2.366, 2.210, and 2.060, and substitution into eqs 3 and 4 yields

(30) Maslen, E. N.; Watson, K. J.; Moore, F. H. *Acta Crystallogr.* **1988, *B44***, 102.
(31) Maslen, E. N.; Ridout, S. C. Watson, K. J.; Moore, F. H. *Acta Crystallogr.* **1987, *C44***, 1510.
(32) Massa, W.; Wocadlo, S.; Hitchman, M. A.; Stratemeier, H. Private communication.
(33) Maslen, E. N.; Ridout, S. C. Watson, K. J.; Moore, F. H. *Acta Crystallogr.* **1988,** *C44*, 412.
(34) Fender, E. F.; Figgis, B. N.; Forsyth, J. B. *Aust. J. Chem.* **1986**, *39*, 1023.
(35) Margulis, T. N.; Templeton, D. H.; *Z. Kristallogr.* **1962**, *117*, 344.
(36) Figgis, B. N.; Kucharski, E. S. *Acta Crystallogr.* **1990, *B46***, 577.
(37) Carrington, A.; McLachlan, A. D. *Introduction to Magnetic Resonance*; Harper and Row: New York, 1967; p 207.
(38) Stratemeier, H. and Hitchman, M. A. Unpublished results.

similar estimates of 28% and 24%, respectively, for the fraction of complexes in the upper state.

The fact that the EPR spectrum does not change significantly in the range 1.5−10 kbar shows that the thermal equilibrium is rather insensitive to pressure in this region. However, this is not the case between 1 bar and ∼1.5 kbar. Though the large line width makes it difficult to resolve the signals accurately due to the two higher *g* values in this pressure region (Figure 6a), these appear to coalesce at ∼0.5 kbar. This suggests that—in accordance with Figure 3 and the discussion in the preceeding paragraph—the potential surface of the $Cu(D_2O)_6^{2+}$ group changes smoothly from that associated with the **L** phase to that of the **H** phase within a narrow range of ∼1 kbar. Since the form of the potential surface depends upon the interactions with the surrounding lattice, this implies that the hydrogen-bonding network also changes in such a way that at the intermediate pressures the lattice forces acting on the $Cu^{2+}$ ions lie between the extreme values.

The powder EPR spectrum in the crossover region is characteristic of a tetragonal **g** tensor, but of the "reversed" type with $g_{||} < g_{\perp}$.[1,4] A **g** tensor of this kind is often considered to be indicative of a tetragonally compressed octahedral geometry, and taken in isolation from the spectra at other pressures, this might be assumed for the present compound. The values $g_{||} = 2.060$ and $g_{\perp} = 2.288$ observed for $(ND_4)_2[Cu(D_2O)_6](SO_4)_2$ at 0.5 kbar indicate a rather large orbital contribution to $g_{||}$, however, which contradicts such a supposition (see below). The situation seems to be similar to that reported for $\gamma$-$Cs_2PbCu(NO_2)_6$ ($g_{||} = 2.06$, $g_{\perp} = 2.15$)[39] and (3-chloroanilinium)$_8$[$CuCl_6$][$Cl_4$] ($g_{||} = 2.06$, $g_{\perp} = 2.19$).[40] For these latter compounds, it was initially assumed that the copper(II) complex has a tetragonally compressed octahedral geometry,[39,40] but in both cases it was subsequently shown[41,42] that at the local level, an orthorhombically distorted tetragonally elongated geometry occurs. The corresponding ground state potential surface would be one in which the two minima are energetically equivalent—a situation approximately intermediate between those depicted in Figure 3.

For $(ND_4)_2[Cu(D_2O)_6](SO_4)_2$, the change in the EPR spectrum as a function of temperature and pressure shows quite clearly that the "reversed" EPR signal is due to the averaging of the *g* values associated with the two Cu−O bonds involved in a dynamic equilibrium. At low temperature and 1 bar pressure, the $Cu(D_2O)_6^{2+}$ complex is "frozen" into the lower energy **L** conformation, and the spectrum is characteristic of an elongated tetragonal octahedral geometry with a slight orthorhombic distortion, producing a signal with $g_{||} > g_{\perp}$ and $g_{\perp}$ split by the orthorhombic distortion (Figure 6b). As the temperature is raised, a thermal equilibrium with the higher energy conformation is established, and the two higher *g* values correlated with the bonds involved in the equilibrium, become partially averaged (Figure 6a) to give a highly orthorhombic spectrum. Increasing the pressure to ∼0.5 kbar changes the ground state potential surface in the manner described to produce an equal number of the two structural isomers, and the two low-field signals associated with the Cu−O7, Cu−O8 directions coalesce to produce the "reversed" tetragonal **g** tensor. The signal associated with the lowest *g* value parallel to Cu−O9 which is not involved in the dynamic equilibrium is nearly invariant to the changes in both temperature and pressure. The magnitude of the lowest *g* value (2.06) also argues strongly against a tetragonally compressed geometry at the local level, as this implies a ground state with the unpaired electron in the $d_{z^2}$ orbital, which would yield a *g* value very close to that of the free electron (2.00). Some enhancement of the *g* value might occur by admixture of the $d_{x^2-y^2}$ orbital into the ground state by vibronic coupling, but this would decrease substantially on cooling,[5] making the lowest *g* value temperature dependent, in contrast to experiment. At about 1.5 kbar the situation described by the potential energy diagram in Figure 3 (**H**) is reached, where the conformation with the longest bonds occurring to O7 is energetically more favorable.

The invariance of the EPR spectrum over the pressure range 1.5−10 kbar at 303 K suggests that the thermal component of the structural equilibrium is essentially unaffected by pressure. This aspect was further investigated by measuring the pressure dependence of the EPR spectrum of ∼2% $Cu^{2+}$ doped into $K_2[Zn(H_2O)_6](SO_4)_2$. The $Cu(H_2O)_6^{2+}$ ion in this host also exhibits a dynamic equilibrium between two structural forms as depicted in Figure 3.[7,9] No change in the EPR spectrum was observed at 300K between 1 bar and 10 kbar, showing that here as well the thermal equilibrium is unaffected by pressure in this range.

The EPR spectrum of powdered $K_2[Cu(H_2O)_6](SO_4)_2$ also showed little change at 301 K between 1 bar and 11.6 kbar (Figure 7b). At 1 bar, values of $g_1 = 2.385$, $g_2 = 2.161$, and $g_3 = 2.057$ were observed, these changing progressively to $g_1 = 2.360$, $g_2 = 2.208$, and $g_3 = 2.043$ at 11.6 kbar. This conforms with the fact that no switch to a high pressure phase was observed by diffraction methods for this compound. However, the significantly enhanced orthorhombicity might indicate that the **L** structure changes slightly toward the **H** lattice. At 1 bar, the two higher *g* values are also observed to diverge on cooling to 113 K, to $g_1 = 2.411$, $g_2 = 2.116$, and $g_3 = 2.053$. This is again consistent with the presence of the thermal equilibrium suggested by the X-ray data. Substitution into eqs 3 and 4 implies that 12 ± 3% of the complexes are in the high energy form, respectively, in reasonable agreement with the estimate of ∼16% from the differences in the bond lengths.

### 3. General Conclusions Regarding the Pressure Switch

The fact that $(NH_4)_2[Cu(H_2O)_6](SO_4)_2$ and its deuterated analogue adopt different structures at 1 bar is quite unusual. It was suggested by Hathaway and Hewat that this might be due to a difference in the hydrogen-bonding capacity of the two isotopes.[11] However, a detailed comparison of hydrogen-bonding interactions in deuterated and hydrogenous compounds has shown that significant differences only occur for very strong hydrogen bonds and that where the distance between the bridged atoms is similar to that in the present compounds, ∼3.0 Å, there is no significant isotope effect.[43] The only other example of a significant structural difference between a deuterated compound and its hydrogenous analogue of which we are aware, is a dicyanoquinonediimine copper(II) complex which behaves as an "organic metal". Here, it was suggested[44] that the structural and concomitant electronic difference accompanying deuteration is probably due to packing effects associated with the small difference between the covalent radius of hydrogen and deuterium, the C−D bond distance being expected to be

(39) Harrowfield, B. V. *Solid State Commun.* **1976**, *19*, 983.
(40) Tucker, D.; White, P. S.; Trojan, K. L.; Kirk, M. L.; Hatfield, W. E. *Inorg. Chem.* **1991**, *30*, 823.
(41) Reinen, D. *J. Solid State Chem.* **1980**, *32*, 311.
(42) Stratemeier, H.; Wagner, B.; Krausz, E. R.; Linder, R.; Schmidtke, H.-H.; Pebler, J.; Hatfield, W. E.; ter Haar, L.; Reinen, D.; Hitchman, M. A. *Inorg. Chem.* **1994**, *33*, 2320.
(43) Hadzi, D. *Hydrogen Bonding*; Pergamon Press: New York, 1959; p. 45.
(44) Sinzger, K.; Hünig, S.; Jopp, D.; Bauer, D.; Bietsch, W.; von Schültz, J. U.; Wolf, H. C.; Kremer, R. K.; Metzenthin, T.; Bau, R.; Khan, S. I.; Lindbaum, A.; Lengauer, C. L.; Tillmanns, E. *J. Am. Chem. Soc.* **1993** *115*, 7696.

marginally smaller than the C−H distance.[45] While this may well be true, it is intriguing that both this compound and the ammonium Tutton salts involve copper(II). In the case of the Tutton salts, an alternative explanation is possible, namely, that the structural difference may be due to the fact that for this metal ion the molecular geometry is strongly influenced by Jahn−Teller coupling. This means that the geometry of the $Cu(D_2O)_6^{2+}$ complex is influenced by the Jahn−Teller active vibration, and hence the ligand mass.

When expressed in dimensionless units, the Jahn−Teller radius $\rho$ is related to the linear Jahn−Teller coupling constant $A_1$ and the energy of the Jahn−Teller vibration ($h\nu$) by the relationship[5,9]

$$\varrho(\text{dimensionless}) = A_1/h\nu \quad (5)$$

Here, both $A_1$ and $h\nu$ are in $cm^{-1}$, and $\rho$ may be converted to pm by the transformation

$$\varrho(\text{pm}) = \varrho(\text{dimensionless}) \times 580.648/\sqrt{(h\nu \text{M})} \quad (6)$$

where $M$ is the ligand mass in amu. The vibrational energy is given by the expression

$$h\nu = (1/2\pi)\sqrt{(k/M)} \quad (7)$$

where $k$ is the force constant of the vibration and the radial distortion parameter for a centrosymmetric complex is defined to a first approximation as

$$\varrho \approx \sqrt{(2\delta x^2 + 2\delta y^2 + 2\delta z^2)} \quad (8)$$

Here, $\delta$x, $\delta$y, $\delta$z are the bond displacements from their mean value along each cartesian axis. Substitution of the expressions in eqs 5 and 7 into eq 6 indicates tha

$$\varrho(\text{pm}) \propto A_1 k^{3/4} M^{1/4}$$

Assuming that both $A_1$ and $k$ are independent of ligand mass, and substituting 18 and 20 amu for the masses of $H_2O$ and $D_2O$, respectively, implies that $\rho(Cu(D_2O)_6^{2+})/\rho(Cu(H_2O)_6^{2+}) \approx 1.027$. That is, upon deuteration, the radial distortion of the copper(II) hexahydrate complex should increase by ∼3%. Experimentally, comparison of the Cu−O bond lengths in $(NH_4)_2[Cu(H_2O)_6](SO_4)_2$ and $(ND_4)_2[Cu(D_2O)_6](SO_4)_2$ at 15 K and ∼1.5 kbar,[12] where they adopt similar structures, yields the values $\rho(Cu(D_2O)_6^{2+}) = 0.335 \pm 0.003$ Å and $\rho(Cu(H_2O)_6^{2+}) = 0.324 \pm 0.003$ Å (uncertainty limits are based upon Gaussian error limits), giving a ratio ∼1.03. Agreement with theory is good, though the uncertainty is large.

When comparing the local Jahn−Teller distortion of the $CuO_6$ octahedra in the various Tutton salts, it is noticeable that the radial distortion parameter $\rho$ is systematically larger in the **L** compared with the **H** structural modification (Table 9). Here, only low temperature structural data are reported so that the $\rho$-values are not influenced by the thermal population of higher energy states. Normally, as may be seen from Table 6, the low-volume **H** phase is more stable than the higher volume **L** modification. However, when a Jahn−Teller distorted complex is present, a larger distortion will produce a greater Jahn−Teller stabilization energy, and this may explain why the **L** phase is only observed for the cations susceptible to this effect, $Cu^{2+}$ and $Cr^{2+}$.

**Table 9.** Radial Distortion Parameters $\rho$ (Å) for the $CuO_6$ and $CrO_6$ Octahedra in Various Tutton Salts with the **L** and **H** Structures

| | **L** Cu−O8 is long | **H** Cu−O7 is long | ref |
|---|---|---|---|
| 1 $(ND_4)_2[Cu(D_2O)_6](SO_4)_2$ at 15 K | 0.369(3) | | 12 |
| 2 $(ND_4)_2[Cu(D_2O)_6](SO_4)_2$ at 1.5 kbar and 15 K | | 0.335(3) | 12 |
| 3 $(NH_4)_2[Cu(H_2O)_6](SO_4)_2$ at 1.5 kbar and 15 K | | 0.324(3) | 12 |
| 4 $(NH_4)_2[Cr(H_2O)_6](SO_4)_2$ at 84 K | 0.374(1) | | 32 |
| 5 $K_2[Cu(H_2O)_6](SO_4)_2$ at 1.4 kbar and 15 K | 0.390(2) | | this work |

A possible explanation for the structural difference between the hydrogenous and deuterated copper compounds at 1 bar is that lattice forces are so delicately balanced that the slightly larger distortion present for the deuterated complex favors the higher volume structure, while the smaller distortion of the hydrogenous complex favors the lower volume structure. The fact that the two forms are interconvertible by a pressure difference of ∼1 kbar, which represents an energy of only ∼0.18(6) kJ per fomula unit ($\Delta E = P\text{d}V$), shows that the structural phases have very similar lattice energies. Circumstantial evidence in favor of this explanation is provided by the fact that for the analogous chromium(II) compounds, *both* the deuterated and hydrogenous salts adopt the high volume structure **L**.[46] The $Cr(H_2O)_6^{2+}$ ion undergoes a similar Jahn−Teller distortion to that of the copper(II) complex, but the $Cr^{2+}$ ionic radius is slightly larger than that of $Cu^{2+}$. If it is the slightly larger tetragonal elongation present in $Cu(D_2O)_6^{2+}$ compared with $Cu(H_2O)_6^{2+}$ which causes the former complex to crystallize in the **L** phase, then the relatively long Cr-O bonds in $Cr(D_2O)_6^{2+}$ and $Cr(H_2O)_6^{2+}$ could explain why both these complexes crystallize in this modification. If this reasoning is correct, then the hydrogenous and deuterated chromium(II) Tutton salts may both undergo a change to the **H** modification at high pressure, the hydrogenous form switching at a somewhat lower pressure than the deuterated, and we are currently testing this hypothesis experimentally.

**Acknowledgment.** We are grateful to Dr. I. M. Krygin for providing access to EPR and high pressure equipment, and Dr. Mark Riley is thanked for useful discussions. The financial assistance of the Australian Research Commission to M.A.H. is acknowledged. The work at Argonne National Laboratory was supported by the U.S. Department of Energy, Basic Energy Sciences-Materials Sciences, under Contract No. W-31-109-ENG-38.

**Supporting Information Available:** Table giving experimental details of the structural determinations (1 page). Ordering information is given on any current masthead page.

IC950857A

(45) Bartell, L. S.; Kuchitsu, K.; DeNeuiR. J. *J. Chem. Phys.* **1961**, *35*, 1211. Greer, S.; Meyer, L. *J. Chem. Phys.* **1970**, *52*, 468.

(46) Figgis, B. N.; Kucharski, E. S.; Reynolds, P. A. *Acta Crystallogr.* **1991**, *C47*, 419.